HALO FORMATION AND EMITTANCE GROWTH DURING BUNCH COMPRESSION OF HIGH-CURRENT HEAVY ION BEAMS

Takashi KIKUCHI and Kazuhiko HORIOKA[1)]

Department of Electrical Engineering, Nagaoka University of Technology, Nagaoka, 940-2188, Japan
[1)] *Department of Energy Sciences, Tokyo Institute of Technology, Yokohama, 226-8502, Japan*

(Received: 17 September 2008 / Accepted: 23 February 2009)

A generation of halo particles and an emittance growth are investigated numerically for a high-current beam transport during a longitudinal bunch compression. The halo particles are generated during the drift compression with an alternating gradient confinement lattice in the transverse direction. The emittance growth is caused by the halo particle generation, and depends on the drift length for the bunch compression. The orbit of generated halo particles extends outward with the beam current increase. The initial particle distribution affects the halo particle generation after the drift beam transport.

Keywords: Space-Charge-Dominated Beams, Heavy Ion Inertial Fusion, Longitudinal Bunch Compression, Halo Particle, Emittance Growth

1. Introduction

In fields of Warm Dense Matter (WDM) sciences, High Energy Density Physics (HEDP), and inertial confinement fusion based on ion beam heating, the large ion beam power should be focused in a local volume of a target to make the higher energy density state [1]. The input power is proportional to the production of the kinetic energy and the beam current. Since the high-current ion beams are needed for the applications, the physics and dynamics of space-charge-dominated beams are crucial issues in WDM, HEDP, and heavy ion inertial fusion researches.

At the final stage of the particle accelerator system, the ion beam pulse should be longitudinally compressed to 10-100 ns. For the effective target experiments, we must compress and transport the ion bunch with the emittance growth less than an allowable level. In a case of the intense ion beam propagation, a particle dilution in the phase space can cause the emittance growth, because the collective relaxation from a non-equilibrium particle distribution to a more thermalized state [2].

We investigate the halo particle generation and the behavior during the longitudinal bunch compression using multi-particle numerical simulations. The halo particles may be a source of the particle loss and emittance growth [3, 4]. The halo particles are generated due to the non-linear self-field during the bunch compression, and cause a large emittance growth in the drift transport. Also, we research the dependence on the initial distribution.

author's e-mail: tkikuchi@nagaokaut.ac.jp

2. Calculation Parameters, Bunch Compression, Transverse Focusing, and Initial Distribution Models

The beam parameters are assumed as Table 1. The initial generalized perveance is assumed to be

Table 1 Beam parameters.

Ion species	Pb^{1+}
Number of ions	6.25×10^{14}
Particle energy [GeV]	10
Initial beam current I_0 [A]	400
Final beam current [kA]	10
Initial pulse duration [ns]	250
Final pulse duration [ns]	10

$Q_i = 3.58 \times 10^{-6}$. The initial emittance ε_i is assumed to be ε_i =10 mm-mrad, and $\varepsilon_{x,rms} = \varepsilon_{y,rms} = \varepsilon_i$. The initial undepressed and depressed phase advances are $\sigma_0 = 72$ deg and $\sigma \sim 65.2$ deg at one lattice period $L_p = 3$ m in the longitudinal direction. The transverse calculation region is fixed at the square of 10 cm $\times$ 10 cm, and the outer boundary condition is given as a conductor wall.

We use a two-dimensional (2D) calculation code in the transverse cross-section with the current increase model for the longitudinal bunch compression [5, 6], which is based on a particle-in-cell (PIC) method [7], takes into account of a self-electrostatic and an external applied magnetic fields. The beam current increase, which is modeled to be as the increase of the statistical weight of the macro-particles, can be given as $1/\left[1 + (1/R_c - 1)s/N_d\, L_p\right]$ in this study. Here s is the transport distance, R_c is the final bunch compression ratio, and N_d is the number of the focusing

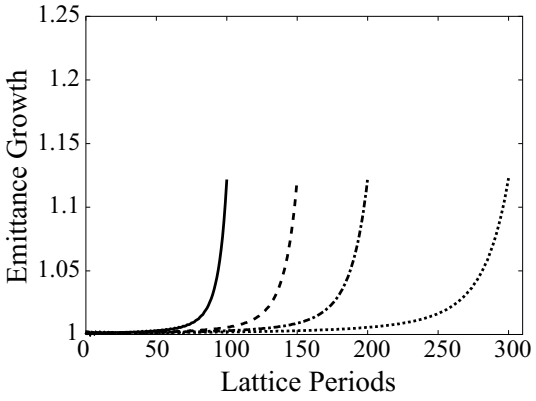

Fig. 1 Emittance growth during drift compression with CF lattice. The lines show the results for the compression length of 100 lattice periods (solid), for the compression length of 150 lattice periods (dashed), for the compression length of 200 lattice periods (dashed and dotted), and for the compression length of 300 lattice periods (dotted), respectively.

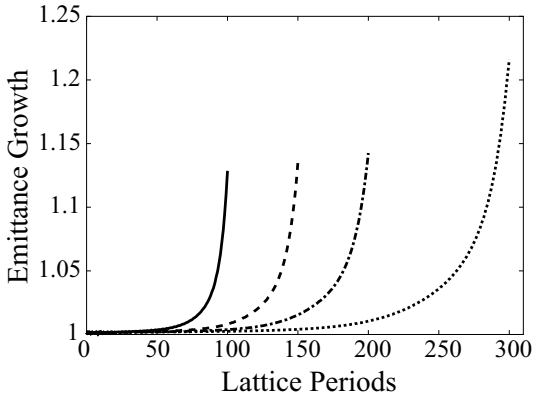

Fig. 2 Emittance growth during drift compression with AG focusing lattice. The lines show the results for the compression length of 100 lattice periods (solid), for the compression length of 150 lattice periods (dashed), for the compression length of 200 lattice periods (dashed and dotted), and for the compression length of 300 lattice periods (dotted), respectively.

lattices for the drift compression. The particle motions are calculated with gamma-factor corrections as the effect of a self-magnetic field [8, 9].

For the beam transport, the transverse confinement scheme is required. In this study, we assumed the continuous focusing (CF) and the alternating gradient (AG) focusing models [8].

The rms matched beams [10, 11] are assumed as the initial particle (non-stationary) distribution for the transverse plane.

3. Emittance Growth and Halo Particles

The emittance value can be useful to evaluate the beam quality. We define the average of unnormalized rms transverse emittance as

$$\varepsilon = \frac{\varepsilon_{x,rms} + \varepsilon_{y,rms}}{2}, \tag{1}$$

where $\varepsilon_{x,rms}$ and $\varepsilon_{y,rms}$ are the unnormalized rms emittances for horizontal and vertical directions given by

$$\varepsilon_{x,rms} = \left[\langle x^2\rangle\langle x'^2\rangle - \langle xx'\rangle\right]^{1/2}, \tag{2}$$

and

$$\varepsilon_{y,rms} = \left[\langle y^2\rangle\langle y'^2\rangle - \langle yy'\rangle\right]^{1/2}, \tag{3}$$

where the prime ($\prime$) indicates the slope, i.e., $x' = dx/dz$ and $y' = dy/dz$.

Figure 1 shows the emittance growth during the bunch compression with CF lattice at each drift transport length. Figure 2 shows the emittance growth during the bunch compression with AG focusing lattice at each drift transport length. In both cases, the Gaussian distribution was assumed as the initial condition in the cross section of the beam.

The Poincaré plots in the transverse direction at each interval of lattice periods are shown in Fig. 3 for the CF, and are shown in Fig. 4 for the AG focusing system, respectively. Only the particles in the low density region are plotted in these figures. Although, Figure 3 indicates the beam transport without any halo generations in the CF, as shown in Fig. 4 the drift compression with the AG focusing system can cause the halo generations.

Figure 4 shows the halo particles are isolated at the six islands in the phase space. It is guessed that the halo particles are originated from the nonlinear space charge force, and are caught in a nonlinear resonance due to the resonance overlaps [12, 13, 14, 15]. Figure 4 shows the orbit extension of halo particles along the beam transport, because the radius of the beam core increases with the beam current increase during the bunch compression. The larger orbit of halo may cause the beam loss.

From the viewpoint of the comparison between Figs. 1, 2, 3, and 4, the emittance growth in the beam transport with the AG focusing system is the result due to the halo particles.

4. Halo Generation Dependence on Initial Distributions

Figure 5 shows the impages for Gaussian (Fig. 5(a)) and parabolic (Fig. 5(b)) distributions in the transverse direction.

For the initially Gaussian distributed and parabolic distributed beams, Figure 6 shows the emittance growth during the bunch compression. The

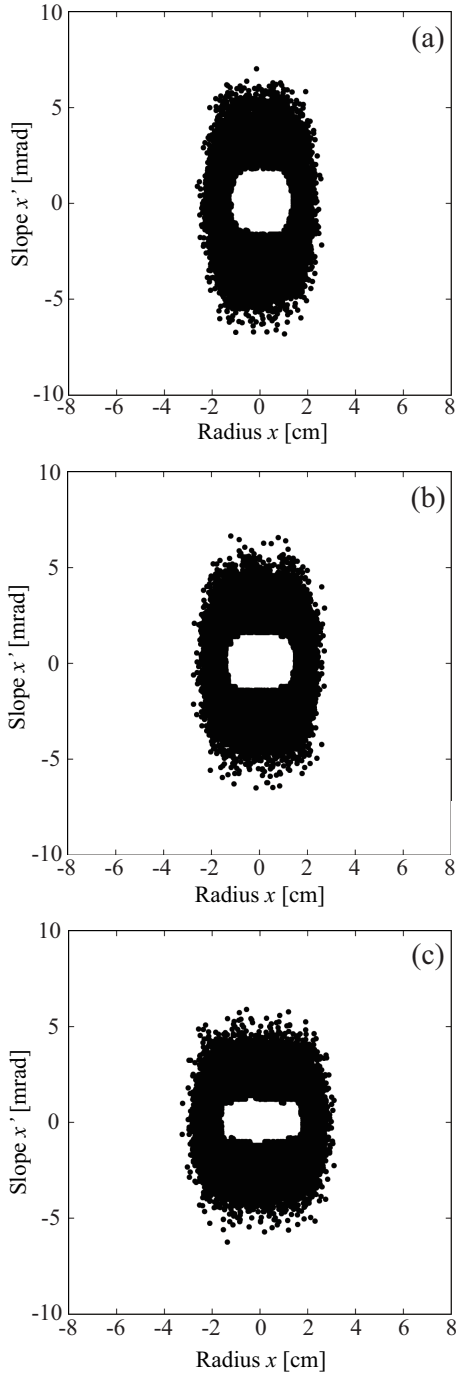

Fig. 3 Poincaré plots in the transverse phase space at the compression length of 300 lattice periods with CF lattice configuration, (a) for the particle projection during 271-280 lattice periods, (b) for the particle projection during 281-290 lattice periods, and (c) for the particle projection during 291-300 lattice periods, respectively. Only the beam particles in the low density regime are plotted.

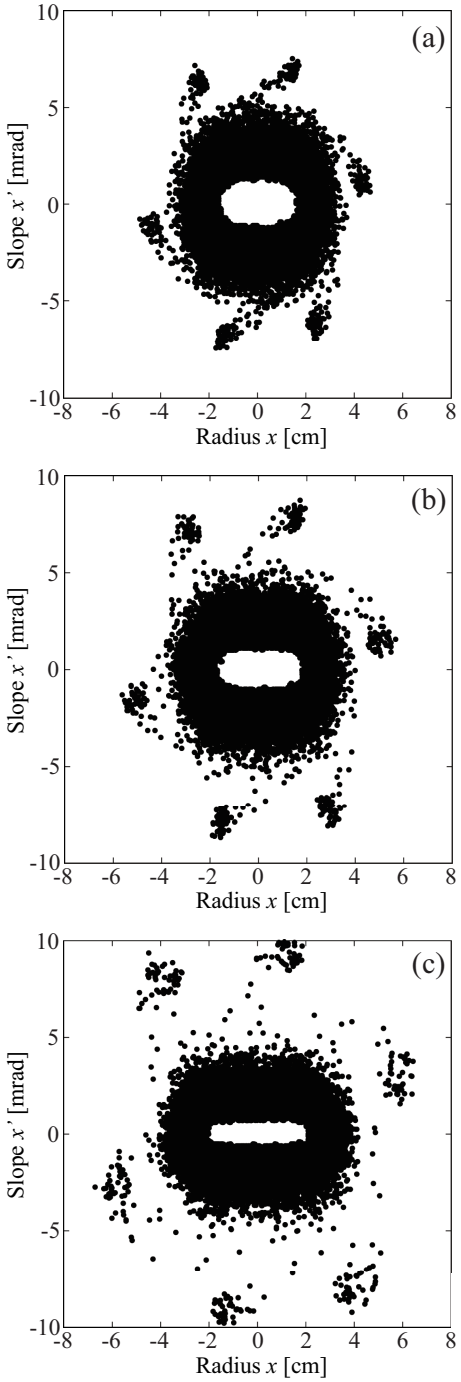

Fig. 4 Poincaré plots in the transverse phase space at the compression length of 300 lattice periods with AG focusing channel, (a) for the particle projection during 271-280 lattice periods, (b) for the particle projection during 281-290 lattice periods, and (c) for the particle projection during 291-300 lattice periods, respectively. Only the beam particles in the low density regime are plotted.

beam given initially as the parabolic distribution has lower emittance growth in comparison with the initial Gaussian beam.

The beam current increase ratio is limited as 25 at the 300 lattice periods, and after the 300 lattice periods the beam is transported in the drift section without bunch compression. Figure 7 shows the stroboscopic plots of the beam particles in the phase space at 500 lattice periods. The particles outside beam core are distributed in the initial Gaussian distribu-

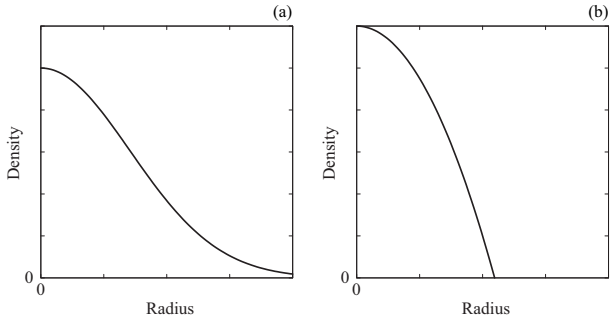

Fig. 5 Aspects of normalized particle distributions, (a) for Gaussian and (b) for parabolic cases.

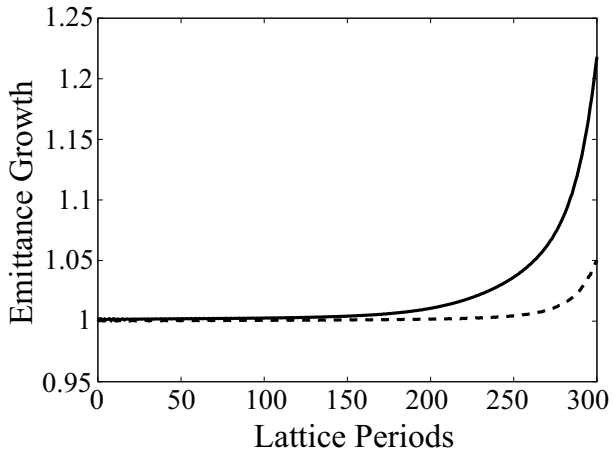

Fig. 6 Emittance growth during bunch compression. The solid curve shows the result for the initial Gaussian distribution. The dashed curve shows the result for the initial parabolic distribution.

tion (Fig. 7(a)), however no halo particles are observed for the initial parabolic distribution (Fig. 7(b)).

5. Conclusion

We studied the halo particle generation and emittance growth during the bunch compression with the high beam current. The orbit of the generated halo particles was extended along the beam transport with the beam current increase. The generated halo particles could contribute to the emittance growth, and the orbit extension of the halo particles is a source of the beam loss. The halo particle generations depended on the initial beam distribution. A Gaussian distribution has a long tail in the distribution, however a parabolic distribution has not particles in the near edge of the beam.

At the edge of the Gaussian distribution, the beam particle has the various betatron oscillation frequencies along the beam transport. The resonance overlapping must produce the halo generation. When the particle distribution can be controlled at the near initial state, the halo particle generation can be suppressed in the drift compression of the high-current beams.

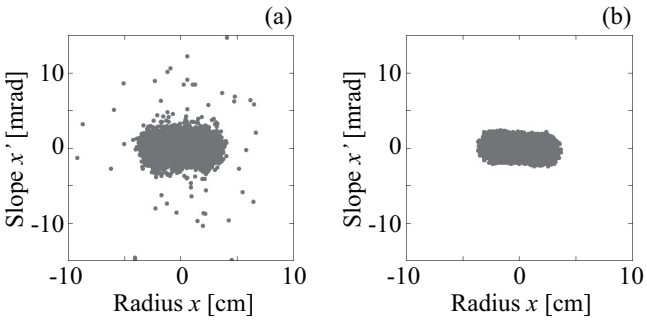

Fig. 7 Particle map in the transverse phase space, (a) for the initial Gaussian and (b) for the initial parabolic distributions.

Acknowledgments

We would like to thank Dr. S.M. Lund for his fruitful discussions and advices.

[1] K. Horioka, T. Kawamura, M. Nakajima, T. Sasaki, K. Kondo, Y. Yano, T. Ishii, M. Ogawa, Y. Oguri, J. Hasegawa, S. Kawata, T. Kikuchi, and K. Takayama, Nucl. Instrum. Methods in Phys. Res. **A 577**, 298 (2007).

[2] S.M. Lund, D.P. Grote, and R.C. Davidson, Nucl. Instrum. Methods in Phys. Res. **A 544**, 472 (2005).

[3] S. M. Lund and S. R. Chawla, Nucl. Instrum. Methods in Phys. Res. **A 561**, 203 (2006).

[4] S. M. Lund, J. J. Barnard, B. Bukh, S. R. Chawla, and S. H. Chilton, Nucl. Instrum. Methods in Phys. Res. **A 577,** 173 (2007).

[5] S.M. Lund, O. Boine-Frankenheim, G. Franchetti, I. Hofmann, and P. Spiller, in *Proceedings of the 1999 Particle Accelerator Conference* (IEEE, Piscataway, NJ 08855, 1999), pp.1785, TUP127.

[6] T. Kikuchi, M. Nakajima, K. Horioka, and T. Katayama, Phys. Rev. ST Accel. Beams **7**, 034201 (2004).

[7] R.W. Hockney and J.W. Eastwood, *Computer Simulation Using Particles*, McGraw-Hill, New York, (1981).

[8] R.C. Davidson and H. Qin, *Physics of Intense Charged Particle Beams in High Energy Accelerators* (World Scientific, New York, 2001),

[9] S. Machida and M. Ikegami, in *Proceedings of the Workshop on Space Charge Physics in High Intensity Hadron Rings* (American Institute of Physics, New York, 1998), p.73.

[10] Y.K. Batygin, Nucl. Instrum. Methods in Phys. Res. **A 539**, 455 (2005).

[11] S.M. Lund, T. Kikuchi, and R.C. Davidson, *submitted to* Phys. Rev. ST Accel. Beams.

[12] J.-M. Lagniel, Nucl. Instrum. Methods in Phys. Res. **A 345**, 405 (1994).

[13] M. Ikegami, Phys. Rev. **E 59**, 2330 (1999).

[14] T. Kikuchi, M. Nakajima, and K. Horioka, Laser Part. Beams **20**, 589 (2002).

[15] Y. Shimosaki and K. Takayama, Phys. Rev. **E 68**, 036503 (2003).